JOURNAL OF SOLID STATE CHEMISTRY 26, 293–309 (1978)

Infrared and Raman Spectral Interpretations of the Ferroelectric Phases of $NaH_3(SeO_3)_2$ and $NaD_3(SeO_3)_2$*

C. A. CODY,† R. C. LEVITT, AND R. K. KHANNA

Chemistry Department, University of Maryland, College Park, Maryland 20742

AND PHILIP J. MILLER

Department of Chemistry, University of Detroit, Detroit, Michigan 48221

Received December 23, 1977; in revised form April 17, 1978

The infrared and Raman spectra of $NaH_3(SeO_3)_2$ and $NaD_3(SeO_3)_2$ have been recorded from 24 to 300°K. The interpretation, assignments, and analysis of the spectral studies are presented on the paraelectric α phase (proton disordered), ferroelectric β phase (proton ordered) and ferroelectric γ phase (proton ordered). A discussion of a newly proposed proton-triggered phase transition mechanism and a possible origin of the hydrogen-bonded O–H stretching region of KH_2PO_4-type ferroelectrics is given.

Introduction

Ferroelectric behavior in hydrogen-bonded crystals undergoing order–disorder phase transitions is believed to be triggered by ordered arrays of protons cooperatively moving from one side to the other side of the proton's double-minimum potential well (*1–3*). The high-temperature paraelectric phase (disordered phase) is believed to result from rapid proton tunneling between the two minima of this same potential well. Two of the better-known crystal series displaying these features are the alkali dihydrogen phosphates, MH_2PO_4, and the alkali trihydrogen selenites, $MH_3(SeO_3)_2$, where M = Li, Na, K, Rb, and Cs.

* This work was supported by a research grant from the Center of Materials Research, University of Maryland.

† Present address: NL Industries, Highlstown, N.J. 08520.

Although these general features of KDP-type ferroelectrics are supported by a variety of experimental techniques (*4–10*), an adequate description of the proton's role in triggering the order–disorder phase transition has not evolved. A consistent description of the origin of the hydrogen-bonded O–H stretching region of KDP-type crystals is also, in general, lacking.

We have recorded the infrared and Raman spectra of sodium trihydrogen selenite, and its deuterated analog, from 24 to 300°K. The results of this investigation have led to a suggestion of a new proton-triggering phase transition mechanism and a new interpretation of the hydrogen-bonded O–H stretching region in KDP-type crystals. These new interpretations are presented in this article. The authors also present their interpretation and assignments of the infrared and Raman spectra of $NaH_3(SeO_3)_2$ and $NaD_3(SeO_3)_2$.

0022–4596/78/0263–0293$02.00/0

Experimental

Single crystals of $NaH_3(SeO_3)_2$ were grown by slow evaporation of aqueous solutions of Na_2CO_3 and SeO_2, with a molar ratio of 1:4 in each case. For infrared studies, well-developed single crystals of $NaH_3(SeO_3)_2$ were dissolved in absolute methanol, and the resulting solution was deposited upon a 1-in.-diameter KBr sample window and allowed to dry in a nitrogen atmosphere. The KBr sample window was placed in a Cryogenic Technology Inc. (CTI) Model 20 cold cell with a modified sample holder which consisted of a brass ring mounted directly to the cold state. Brass screw-in rings were used to secure the sample window, thus ensuring good thermal contact. The temperature was recorded on a CTI digital temperature indicator driven by a chromal–gold (0.07% iron) thermocouple mounted directly to the brass ring. Calibration of the digital readout was checked against liquid nitrogen, dry ice, and the ice point of water.

For small-temperature-variation experiments, a Fischer temperature controller (Model 22) in conjunction with two Yellow Springs' platinum resistor probes were coupled to the CTI cold cell. With this arrangement, temperatures could be recorded to ± 0.1°K.

Infrared spectra were recorded on a Digilab FTS-14 spectrophotometer over the region 4000 to 450 cm^{-1}. All spectra were ratio plotted, with 100 scans of the cold cell and blank sample window used as a background spectrum and 100 scans of the cold cell and sample window used as the sample spectrum. All reported infrared spectra were scale expanded by the FTS-14 (i.e., the lowest actual transmission value was set at 0% and the highest actual transmission value was set at 100%) and were then plotted. Periodically, calibration of the FTS-14 was checked with a polystyrene film. Reported infrared frequencies are accurate to ± 2 cm^{-1} for sharp bands and to ± 20 cm^{-1} for broad bands.

Infrared spectra of deuterated compounds were obtained in a similar manner with the exception of sample window preparation. Single crystals of $NaD_3(SeO_3)_2$ were mulled with nujol and deposited on the KBr windows as thin films. This procedure was used because deposition from CH_3OD solutions resulted in ~50% exchange of H for D via atmospheric water. Even the nujol method resulted in a small amount of exchange.

For Raman studies, large transparent crystals of $NaH_3(SeO_3)_2$ were oriented with a polarizing microscope and cut and polished into small cubes ~5 mm on an edge. The oriented cubes were mounted directly to the cold station with optical coupling compound. The optical coupling compound was mixed with powdered copper to ensure good thermal contact. Raman spectra of $NaD_3(SeO_3)_2$ were recorded in a similar manner except that unoriented single crystals were used as samples. This was done because deuterated crystals of a size sufficient to orient were not obtained from the growing solution.

Raman spectra were recorded on a Spex 1401 double monochromator coupled to a Coherent Radiation Model 52 argon ion laser (4880 A, ~500 mW) utilizing 90° scattering. A thin polaroid film was placed between the sample and slits of the monochromator to obtain the various polarizations. The monochromator was calibrated by scanning over nonlasing lines of the Model 52 laser. Reported Raman frequencies are accurate to ± 3 cm^{-1} for sharp bands and to ± 20 cm^{-1} for broad bands.

Discussion

A. Paraelectric Phase (α) of $NaH_3(SeO_3)_2$

The paraelectric phase of $NaH_3(SeO_3)_2$ (α phase) belongs to the space group $P_{2_1/n}$ containing two molecules per unit cell (*11*). Kaplan *et al.* (*12*) carried out a neutron diffraction study of $NaH_3(SeO_3)_2$ in the α phase and found the SeO_3^{2-} ions to be slightly distorted from an ideal pyramid (point group

C_{3v}) resulting from differing bond lengths and angles of the molecule. Their determination of the SeO_3^{2-} geometry was quite close to that reported in Vijayan's (*11*) X-ray study. Each of the above-mentioned structural works suggests a point group symmetry of SeO_3^{2-} close to C_s, although the actual symmetry is C_1.

Kaplan *et al.* (*12*) described the hydrogen bond network as consisting of SeO_3^{2-} ions hydrogen bonded to neighbouring SeO_3^{2-} so that each oxygen is hydrogen bonded to a different SeO_3^{2-} ion. This produces six SeO_3^{2-} ions hydrogen bonded in a closed loop. The proton in hydrogen bond O(1)–H(1)–O(1) (O...O distance, 2.60 Å) appears to be disordered and centered, and the proton in O(2)–H(2)–O(3) (O...O distance, 2.56 Å) appears to be situated closer to O(2) than to O(3); yet the possibility of a broad single-minimum potential well for H(2) is not ruled out. The numerals associated with the O and H atoms are crystallographic designations.

Soda and Chiba (*9*) employed the deuteron magnetic resonance technique to study the deuterium motions and hydrogen bond network above and below the phase transition in $NaD_3(SeO_3)_2$. They concluded that above T_c there are two nonequivalent hydrogen bonds and that the deuterium atoms in these bonds are tunneling rapidly between two sites in their respective double-minimum wells.

Blinc *et al.* (*13*), on the basis of the results of a deuteron magnetic resonance study, reported $NaD_3(SeO_3)_2$ (designated α_D) to be isostructural with $NaH_3(SeO_3)_2$ in the room-temperature phase.

Numerous infrared and Raman spectral studies have been reported for the various phases of $NaH_3(SeO_3)_2$ and $NaD_3(SeO_3)_2$ (*4*, *10*, *14*, *15*). Khanna *et al.* (*10*) (infrared) were the first group to suggest that the 300- to 900-cm^{-1} region of the α phase was very similar to the same spectral region of crystalline Na_2SeO_3; therefore, they concluded that all protons were disordered in the α phase of $NaH_3(SeO_3)_2$. Khanna *et al.* (*10*) further suggested that the low-temperature ferroelectric phase transition was triggered by protons. They based their interpretation upon changes in the frequency of the SeO_3^{2-} vibrations as the transition was crossed.

Although later infrared and Raman studies also confirmed the proton's role in triggering the transition, many questions remained unanswered. In particular, previous spectral studies were not in agreement on the assignments of the internal modes, hydrogen-bonded O–H stretching and bending modes, and the degree of proton order in the different phases (*10*, *14*, *15*).

To clarify the situation, a study of the internal mode frequencies of $*SeO_3^{2-}$, $HSeO_3^-$,

TABLE I

THE STRETCHING (st) AND BENDING (bd) FREQUENCIES (cm^{-1}) OF $*SeO_3^{2-}$, $HSeO_3^-$, AND H_2SeO_3 AND THEIR DEUTERATED ANALOGS[a]

Assignment	$*SeO_3^{2-}$[b]	$HSeO_3^-$[c]	$DSeO_3^-$[c]	H_2SeO_3[d]	D_2SeO_3[d]
$\nu_1(A')$ SeO(1) st	800	602	584	832	832
$\nu_2(A')$ SeO(2, 3) bd	450	408	408	426	408
$\nu_3'(A')$ SeO(2, 3) st	670	867	863	700	686
$\nu_3''(A'')$ SeO(2, 3) st	660	798	801	689	675
$\nu_4'(A')$ SeO(1, 2, 3) bd	335	320	316	359	349
$\nu_4''(A'')$ SeO(1, 2, 3) bd	375	359	359	332	327

[a] Reference (*16*).

[b] SeO_3^{2-} with disordered protons in the lattice.

[c] Frequencies from $LiHSeO_3$ and $LiDSeO_3$, respectively.

[d] Frequencies from selenous acid (H_2SeO_3 and D_2SeO_3, respectively).

and H_2SeO_3 and their deuterated analogs in various alkali hydrogen selenite salts was undertaken (*16*). A summary of these results can be found in Table I.

These results indicated that the ordering of protons caused dramatic frequency shifts in the selenite modes so that the degree of proton order could be followed in this manner. Also, tentative assignments on the various $NaH_3(SeO_3)_2$ phases can be based on these findings.

From the structure reports several molecular units are possible in the α phase. If protons H(2) are ordered, the spectra would be representative of SeO_3^{2-}, $H_2SeO_3^-$, and $HSeO_3^-$ or H_2SeO_3 and SeO_3^{2-}. The simultaneous presence of three molecular units is possible if the H(2) protons order on different SeO_3^{2-} ions in one region and in the other regions of the crystal order on the same SeO_3^{2-} ions. In either case, ordered H(2) protons would produce H_2SeO_3 frequencies in the spectra of the α phase.

If the H(2) protons are disordered, the spectra would be similar to $^*SeO_3^{2-}$ and the bandwidths would be broad because of intermolecular coupling. The lack of characteristic H_2SeO_3 stretching frequencies (ν_1 = 832 cm^{-1}, ν_3' = 700 cm^{-1}, and ν_3'' = 689 cm^{-1}) in the α phase infrared and Raman spectra of Figs. 1 and 2, respectively, in conjunction with the observation of strong broad $^*SeO_3^{2-}$-type stretching frequencies at ν_1 = 800 cm^{-1} and ν_3' and ν_3'' at 660 cm^{-1} in these same figures definitely indicates that all protons are dynamically disordered in the α phase of $NaH_3(SeO_3)_2$.

The structure reports indicate that the paraelectric α phase contains two distinct hydrogen bond lengths of 2.56 Å [O–H(2)–O] and 2.60 Å [O–H(1)–O] (*11*, *12*). Two bending modes are observed in the infrared spectrum (Fig. 1). Making the assumption that the shorter the hydrogen bond length the higher the bending frequency leads us to assign the 1230-cm^{-1} mode as an O–H(2)–O bend and the 1160-cm^{-1} mode as an O–H(1)–O bend.

Peercy (*4*) has assigned the ~1600-cm^{-1} mode as an O–H–O bend, but in consideration of the remarkable similarity of the proton

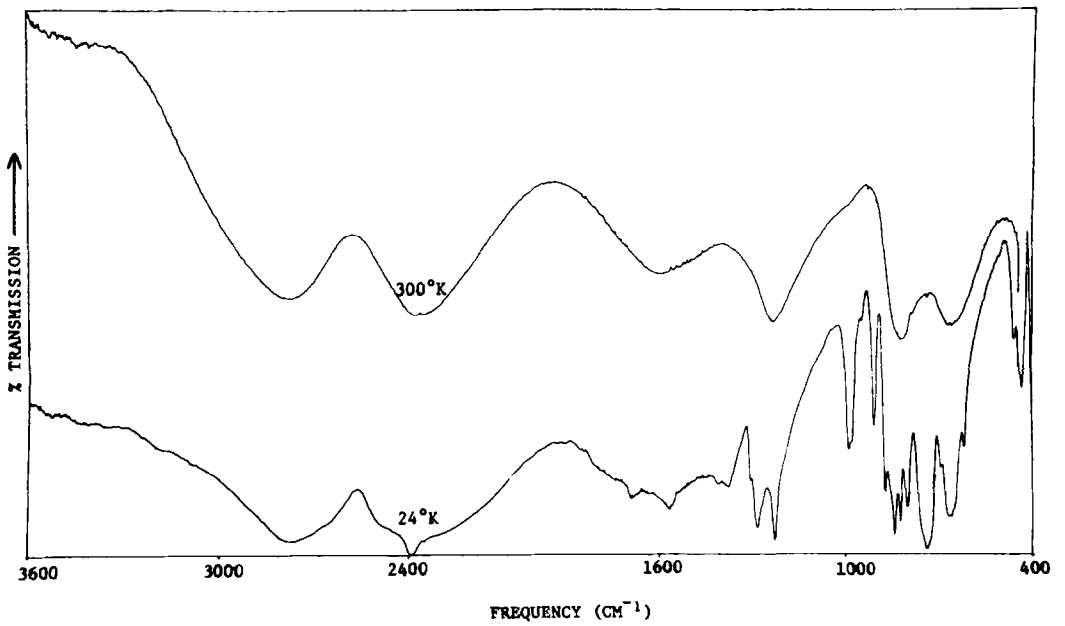

FIG. 1. The infrared spectrum of polycrystalline $NaH_3(SeO_3)_2$ (α-phase upper spectrum and β-phase lower spectrum).

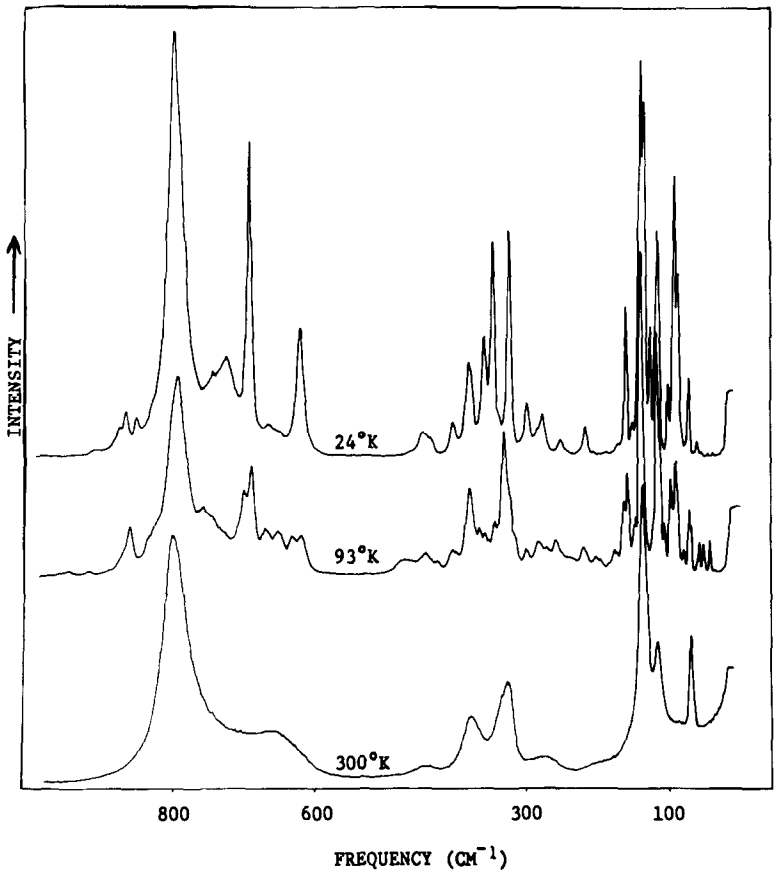

FIG. 2. The $b(cb)a$ Raman spectrum of a $NaH_3(SeO_3)_2$ single crystal in the α phase (300°K), β phase (103°K), and γ phase (24°K).

stretching regions of the alkali dihydrogen phosphates and trihydrogen selenites we have assigned this mode as a proton stretch along with the 2760- and 2360-cm^{-1} modes. The origin of these modes is discussed at length in the next section, entitled "Hydrogen Bond Stretching Region." The frequencies and assignments of the α and α_D phases are found in Table II.

B. First Ferroelectric Phase (β) of $NaH_3(SeO_3)_2$

Pepinsky and Vedam (*5*) have reported a phase transition in $NaH_3(SeO_3)_2$ occurring at 194°K. From 194 to 100°K, $NaH_3(SeO_3)_2$ is a ferroelectric triclinic crystal, space group P_1 (β phase) with eight molecules per unit cell resulting from a doubling of the α phase unit cell in the a and b directions (*20*). No X-ray diffraction studies have been reported on the β phase, although optical (*17*), dielectric (*18*, *19*), nuclear magnetic resonance (*20*, *21*), and specific heat (*8*, *22*) data are known. $NaD_3(SeO_3)_2$ does not have an equivalent β_D phase, the low-temperature phase of $NaD_3(SeO_3)_2$, which has a transition temperature of 272°K, is monoclinic with space group Pm (γ_D phase) and is ferroelectric (*20*). The spectra of the γ_D phase of $NaD_3(SeO_3)_2$ are, therefore, discussed under the γ phase of $NaH_3(SeO_3)_2$.

The authors feel that the $\alpha \rightarrow \beta$ phase transition can be visualized as resulting from an

TABLE II

THE INFRARED AND RAMAN FREQUENCIES OF THE α AND α_D, PHASES

	$NaH_3(SeO_3)_2$					$NaD_3(SeO_3)_2$ unoriented[a]				
		Raman					Raman			
Assignment	ir	$b(aa)c$	$b(ab)c$	$b(cc)a$	$b(cb)a$	ir	pol.$_{\perp}$	depol.	pol.$_{\parallel}$	depol.
Hydrogen bond stretching region	2760	2710		2780		2070	2060		2075	
	2360	2310		2340		1750	1760		1750	
	1600	1600		1600		1250	1280		1290	
						980				
δ_1 and δ_0 hydrogen bond bending	1230	1200		1250		920				
	1160							874		875
$\nu_1(A')$ $^*SeO_3^{2-}$	820	803	796	803	801	830	813	812	812	813
$\nu_3'(A')$ $^*SeO_3^{2-}$	660	684	696	668	660				700	696
$\nu_3''(A'')$ $^*SeO_3^{2-}$						660	653	659		657
$\nu_2(A')$ $^*SeO_3^{2-}$	425	443			448		431	435	420	436
$\nu_4(A'')$ $^*SeO_3^{2-}$	359	391	385	385	386			381	375	
$\nu_4'(A')$ $^*SeO_3^{2-}$	324	337	345	331	331		344	336	338	333
O...Oν_s stretching region	249	261	259	280	283		250	249		
	242									
Lattice region		182	163	186			158		160	
		143		140	139		133		133	
		120	118	122	120		110	113	110	113
								94	93	92
		74	73	73	74		70	70	70	69
			62							

[a] I and II are two different crystal orientations.

ordering of H(2) protons, with the remaining H(1) proton disordered. This point is discussed below.

Makita and Miki's (*22*) heat capacity data indicated $\Delta S = 1.03$ e.u. for the $\alpha \rightarrow \beta$ transition. The $\beta \rightarrow \gamma$ transition is accompanied by $\Delta S = 0.5$ e.u. or overall, the $\alpha \rightarrow \beta \rightarrow \gamma$ value for ΔS is 1.53 e.u. The magnitude of the reported phase transition entropy found in $NaH_3(SeO_3)_2$ and $NaD_3(SeO_3)_2$ indicates that these phase transitions are of the order–disorder type.

It is not unreasonable to attribute the entire phase transition entropy solely to changes in the proton position (*23*); therefore, if the ordering is complete for the $\alpha_D \rightarrow \gamma_D$ transition ($\Delta S = 1.58$ e.u.), then one expects each proton to contribute $\Delta S \simeq 0.5$ e.u. to the transition entropy. Evidence of total deuteron order in the γ_D phase has been presented by Soda and Chiba (*9*) (DMR), by Torrie and Knispel (*14*), (Raman), and by the present authors (see next section). The entropy argument would then imply that the $\alpha \rightarrow \beta$ transition entropy of 1 e.u. for $NaH_3(SeO_3)_2$ results from an ordering of two protons, leaving the third proton disordered.

Torrie and Knispel (*14*) previously indicated that the Raman spectra of the β phase suggest this phase to be more disordered than the γ phase. Their interpretation of the spectra was based upon the assumption that all protons in the β phase were disordered, but more ordered than in the α phase. They gave no explanation for a ferroelectric phase composed only of disordered protons.

The β phase has two polarization directions. One direction is the b axis, and the other is in the a–c plane (*17*). As was pointed out in the discussion on the α phase, the ordering of H(2) protons could occur on the same or different SeO_3^{2-} ions throughout the crystal. The molecular units $HSeO_3^-$, H_2SeO_3, and SeO_3^{2-} would then be present, and polarization reversal in both directions is realized by cooperative switching of protons on $HSeO_3^-$ and on H_2SeO_3.

In the infrared and Raman spectra of the β phase of $NaH_3(SeO_3)_2$ (Figs. 1 and 2, respectively), frequencies characteristic of SeO_3^{2-}

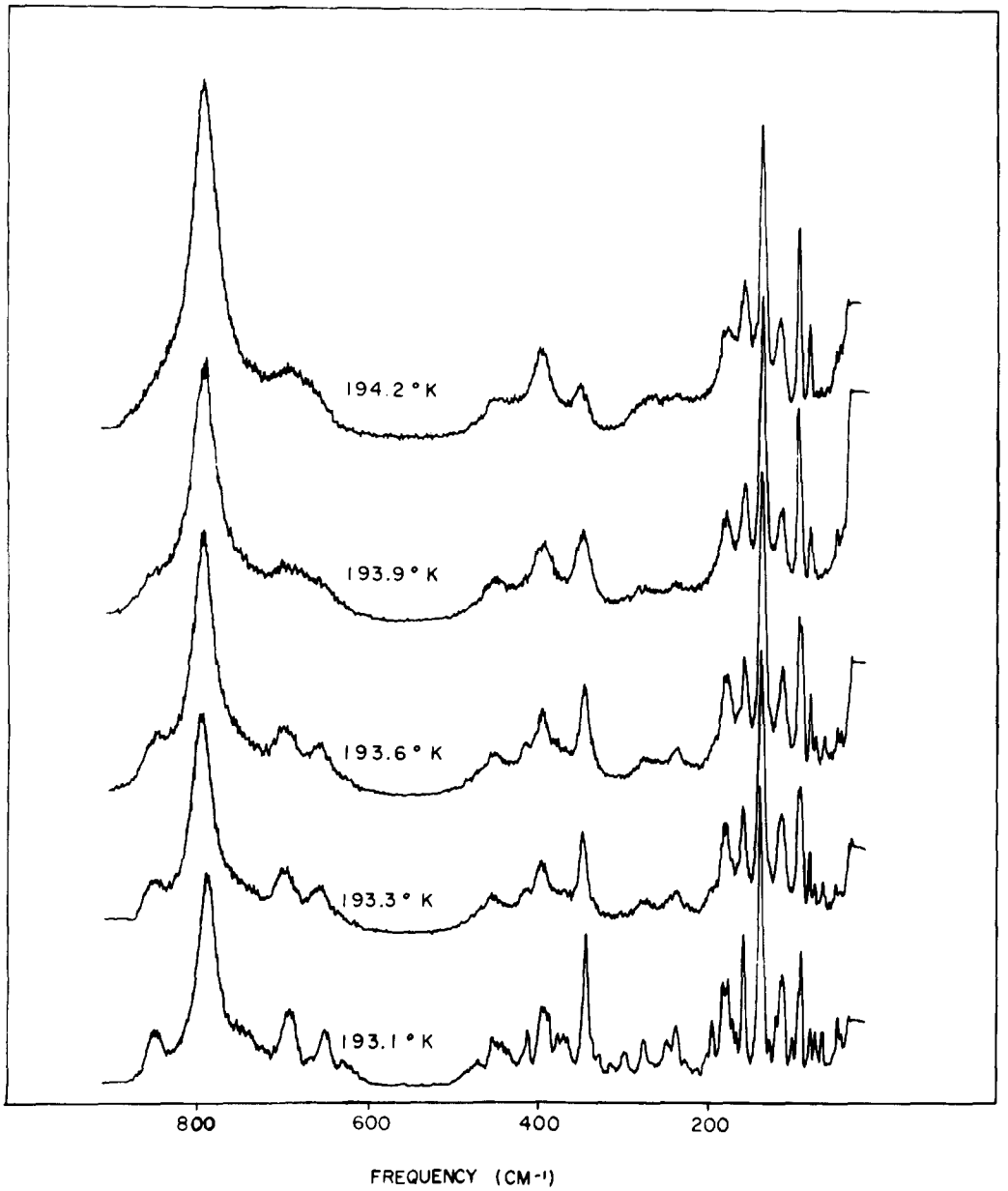

FIG. 3. Temperature variations in the $b(cb)a$ Raman spectrum of $NaH_3(SeO_3)_2$ in the $\alpha \rightarrow \beta$ phase transition region.

TABLE III

THE INFRARED AND RAMAN FREQUENCIES OF THE β PHASE ($T = 113°K$)

Assignment	ir	$b(aa)c$	$b(ab)c^a$	$b(cc)a$	$b(cb)a^a$
Hydrogen bond stretching region	2760			2760	
	2660				
	2480				
	2395	2340		2380	
	1898				
	1845				
	1792				
	1738				
	1685	1655			
	1595			1600	
	1560	1550			
δ_1 and δ_0 hydrogen bond bending	1410				
	1365				
	1340				
	1305				
	1282			1290	
	1268	1245			
	1228	1198		1235	
	998				
	980				
	960	955	954	951	952
	950				
	910			922	
$\nu_1(A')H_2SeO_3$	878				876
	860	863	867	865	864
$\nu_3'(A')HSeO_3^-$	848	843			
	829	825			830
$\nu_3''(A'')HSeO_3^-$ and $\nu_1SeO_3^{2-}$	805	798	795	798	799
$\nu_3'(A')H_2SeO_3$	748		753	762	760
	732				
$\nu_3''(A'')H_2SeO_3$	695	694	703	705	707
				697	698
	680			672	675
$\nu_3'(A')$ and $\nu_3''(A'')SeO_3^{2-}$	670			660	
	650	651	655	655	659
				639	
$\nu_1(A')HSeO_3^-$	625			626	626
$\nu_2'(A')HSeO_3$	465	470	482	485	467
				477	
		466	451	451	453
$\nu_2(A')H_2SeO_3$	439	430	431	433	
	410	415		410	415
$\nu_2(A')H_2SeO_3$	402	406	407		
			393		
	388	385	386	389	390
	377	373	373	371	373
$\nu_4'(A')H_2SeO_3$	373				
	360	365	369		368

TABLE III—*Continued*

Assignment	ir	$b(aa)c$	$b(ab)c$[a]		$b(cb)a$[a]
$\nu_4''(A'')H_2SeO_3$	354	352		351	351
	350				
	346	339	340	340	340
$\nu_4'(A')HSeO_3^-$ and SeO_3^{2-}	338, 327		330	330	
	323, 318			324	
O...O ν_s stretching region	304	306	306	308	309
	209, 280	283		280	
	262	266	270	268	265
	254		253	246	
	239		241		243
	215	207	228	211	229
	208		213		
Lattice region		190	203	193	202
		184	181	183	181
		167	167	170	171
		162	164	166	166
		156	154	152	153
			152		
		143	143	143	143
		122	132	122	122
			123		
		115		112	114
		110	110		
		103	103	104	103
		94	95	95	98
		85	83	88	86
		78	75	77	79
		73	73	72	76
		63	62	63	61
		56	53	56	58
		46	46	47	
		43			
		35			

[a] The 1000- 3000-cm^{-1} regions of these orientations were not recorded.

(800 cm^{-1}), $HSeO_3^-$ (630 and 860 cm^{-1}), and H_2SeO_3 (830, 705, and 685 cm^{-1}) are seen, indicating that two protons have ordered. Torrie and Knispel's suggestion of residual disorder in the β can be explained by the presence of the remaining disordered third proton. This residual disorder in the crystal drives the bandwidths of all modes to intermediate values, thus giving the spectra the appearance of more order than the α phase, but less order than the γ phase.

Several groups have concluded that the $\alpha \rightarrow \beta$ phase transition is second order (*17*, *18*), whereas others have indicated that this transition is first order (*20*, *22*). The Raman spectra recorded during the small-temperature-variation experiments indicate that the $\alpha \rightarrow \beta$ phase transition is apparently second order. This conclusion is based upon the continuous spectral charges in the vicinity of T_c (Fig. 3) and the lack of thermal hysteresis upon cooling or heating the sample. The frequencies and assignments of the β phase are listed in Table III.

C. Second Ferroelectric Phase (γ) of $NaH_3(SeO_3)_2$

Makita *et al.* (*22*) reported a second phase transition in $NaH_3(SeO_3)_2$ which occurred at about 100°K. Below 100°K, $NaH_3(SeO_3)_2$ is monoclinic, space group *Pm*, with four molecules per unit cell, resulting from a doubling of the α phase unit cell in the *a* direction only (*20*). Optical (*17*), heat capacity (*8*), dielectric (*14*, *24*), NMR (*20*, *21*), and Raman (*4*, *14*, *15*) studies have been reported for the γ phase. $NaD_3(SeO_3)_2$ undergoes a phase transition at 272°K, from the α_D to the γ_D phase without the appearance of the β_D phase (*13*). Soda and Chiba's (*9*) DMR study below 272°K suggested the existence of asymmetric double-minimum potentials for the three hydrogen bonds connecting each SeO_3^{2-} ion. Complete ordering of all protons was also proposed for the γ_D phase.

The Raman spectra immediately below the $\beta \rightarrow \gamma$ transition (Fig. 2) is characterized by the appearance of intense $HSeO_3^-$ bands replacing the β phase SeO_3^{2-} bands and by some rearrangement of the H_2SeO_3 frequencies. The rearrangement of H_2SeO_3 frequencies probably results from changing Se–O bond lengths and force constants as the third proton orders. The appearance of $HSeO_3^-$ bands and the corresponding disappearance of $^*SeO_3^{2-}$ bands indicate that the remaining proton is ordered. The γ phase of $NaH_3(SeO_3)_2$ then contains ordered protons only.

In passing into the γ phase, the *b* component of polarization disappears (*17*). The *a*–*c* polarization component of the β phase remains in the γ phase and retains its value as the transition is crossed (*17*), which is expected if the hypothesis of two ordered protons in the β phase is accepted. This results from a completely ordered network of protons. As protons are switched across the barrier they must all move into the opposite minimum, and since there are only two stable positions only one direction in the crystal can be ferroelectric.

Khanna *et al.* (*10*) recorded infrared spectra below the $\beta \rightarrow \gamma$ transition temperature, but they saw no spectral changes associated with a phase transition. Similarly, Torrie and Knispel (*14*) observed no changes in the infrared spectra at the $\beta \rightarrow \gamma$ transition. The authors repeatedly tried to detect $\beta \rightarrow \gamma$ phase transi-

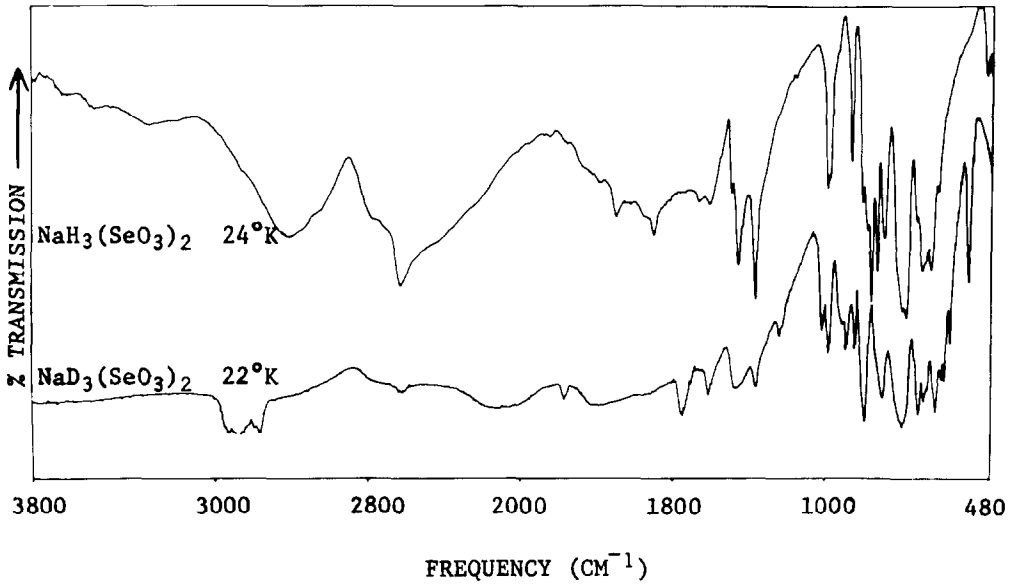

FIG. 4. Comparison of the infrared transmission spectra of the β and γ_D phases of $NaH_3(SeO_3)_2$. (* denotes nujol bands.)

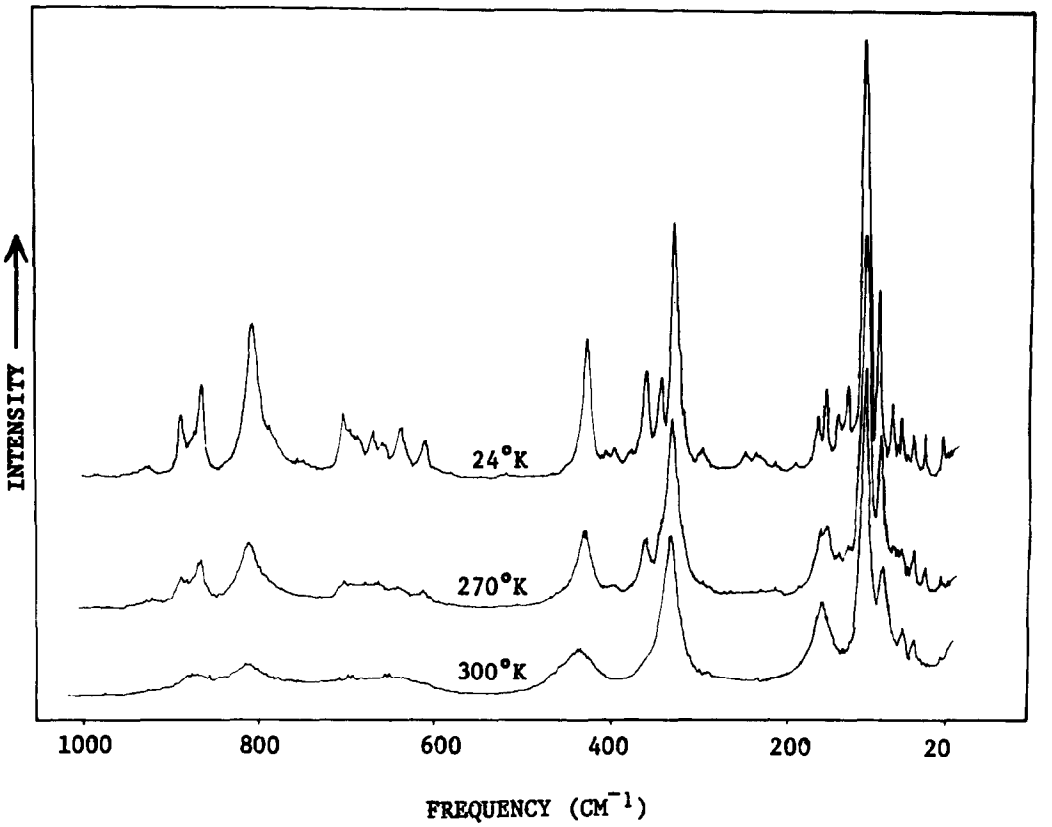

FIG. 5. Raman spectrum of unoriented $NaD_3(SeO_3)_2$ single crystal at 300, 270, and 24°K.

tions by using infrared spectroscopy. The samples were cycled around the transition temperature, and they were maintained 1 or 2°K below the $\beta \rightarrow \gamma$ transition for up to 24 hr, to allow for a sluggish phase change; all attempts, however, were unsuccessful.

It is possible that these differences in the infrared and Raman spectra are due to different sample forms, i.e., polycrystalline versus single crystal, but this would seem to be eliminated by the work of Torrie and Knispel (*14*), who observed the $\beta \rightarrow \gamma$ transition in the Raman spectra recorded off of a pellet pressed from powdered $NaH_3(SeO_3)_2$.

To complicate matters, the β phase of $NaH_3(SeO_3)_2$ and the γ_D phase of $NaD_3(SeO_3)_2$ yield similar infrared spectra (Fig. 4); yet Raman spectra of the β and γ_D phases are quite different (Figs. 2 and 5, respectively). Before an interpretation of this feature can be given, additional research must be carried out.

The low-frequency Raman spectra for the $\beta \rightarrow \gamma$ transition is presented in Fig. 6. The transition is thought to be first order based upon the discontinuous spectral changes at T_c. A large thermal hysteresis of approximately 15.4°K was noticed upon heating the sample in the γ phase.

The frequencies and assignments of the γ and γ_D phases can be found in Table IV.

Mechanism of the Transition

To discuss the mechanism of the phase transition from the disordered to the ordered state, an examination of the proton's energy level scheme in the double-minimum potential with a low intrabond barrier is in order. The proton's energy system can be described as

TABLE IV

THE INFRARED AND RAMAN FREQUENCIES OF THE γ AND γ_D PHASES ($T = 24°K$)

	$NaH_3(SeO_3)_2$					$NaD_3(SeO_3)_2$[a] unoriented[b]				
		Raman					24°K Raman			
Assignment	ir	*b*(*aa*)*c*	*b*(*ab*)*c*	*b*(*cc*)*a*	*b*(*cb*)*a*	ir	pol.$_I$	depol.	pol.$_{II}$	depol.
Hydrogen bond stretching	2760	2710		2780		2070	2090		2070	
	2660						2020			
	2480					1850	1855		1855	
	2395	2350		2400		1760	1770		1765	
	1898									
	1845					1580				
	1792									
	1738									
	1685	1650				1285	1300		1294	
	1595			1580		1220	1232		1220	
	1560	1528				1148	1155		1150	
	1410									
	1365			1375			1025			
δ_I and δ_0 hydrogen bond bending	1340					1008	1005			
	1305			1310		985	988			988
	1282	1250		1275		940				982
								930	930	
	1268	1230				928				
	1228	1190		1230		899	897		892	892
	988		988			611	617	617	618	
	980		985			602	604	603	600	
	960	952				583	590	598	583	
	910	912	911	912	910	522	531	530	520	522
$\nu_1(A')H_2SeO_3$	878	872				870	874	873	881	878
	860					862		864	867	868
$\nu_3^I(A')HSeO_3$	848		842	852	851					
	829	838	827		830	825	838	837		
$\nu_3''(A'')HSeO_3^-$							807	807	810	
	805	796	800	795	795	805	798	788		793
$\nu_3^I(A')H_2SeO_3$	748	774	763	750	740					
	732			728	730	705	709	709	708	706
$\nu_3''(A'')H_2SeO_3$	695	701				688	688	692		692
	680	693	700	694	692			688		
$\nu_1(A')HSeO_3^-$	670					670	674	676		673
	650	660	655	651	667	660	660	660	661	662
	625	625	630	628	623	630	640	643	643	640
$\nu_2(A')HSeO_3^-$	465	455	453	452						
			436	439	440		435	431	435	431
							431			
$\nu_2(A')H_2SeO_3$		403	419	410	410		406	401	413	412
			404				403			402
$\nu_4''(A'')HSeO_3^-$			391	388	386		386	385	386	384
		382	383		386		372	371		
$\nu_4''(A'')H_2SeO_3$		365	345	366	365		359	366		365

TABLE IV—*Continued*

	$NaH_3(SeO_3)_2$				$NaD_3(SeO_3)_2$[a] unoriented[b]				
		Raman				24°K Raman			
Assignment	ir	*b*(*aa*)*c*	*b*(*ab*)*c*	*b*(*cc*)*a*	*b*(*cb*)*a*	ir	pol.$_{I}$	depol.	pol.$_{II}$	depol.
$\nu_4'(A')H_2SeO_3$		352	350	352	352		352	341	341	348
$\nu_4'(A')HSeO_3^-$		330	338	330	328		332	333	333	330
							327	327		
		305	313	305	300		301	301	301	301
				291	290		291	291		290
O...O ν_s stretching			283	286	282		270	270	270	
region		259	258	259	255		256	257	251	
		235	235		230		241	242		243
		223	225	225	223		224	225	220	220
Lattice region		193	194		191		198	203		
		183	183				191	200	190	196
								191		
		173	174		177		178	182	171	171
			171					178		
		163	164	165	165		164	163	161	161
		156	158	156	157		157	159		
		150	150		150		148	150	149	149
		143		145	144		141	145	142	
								141		
		140	141	149	149		132	133	138	136
		132	130	130	130				131	
		122	120	120	121		121	123		
		118	112		119		114	117	119	118
		103	100	107	105		106	103	103	100
				96	97		98	98	98	
		92	92	92	91		94			
			83		86		88	89	88	87
			80				82	82		
		75	74	76	75		76	76	75	74
		64	62	67	65		63	62	64	69
		59		58	58		58	58	55	62
		50	53	50	49		52	52	50	50
		46	46					48		

[a] In the assignment column replace H with D, i.e., $\nu_1(A')H_2SeO_3 \rightarrow \nu_1(A')D_2SeO_3$.

[b] I and II are two different directions of the unoriented crystal.

consisting of a series of discrete levels, each level having its own distinct probability and consequently, frequency, of tunneling. The lowest level has a tunneling frequency of zero, and consequently, the proton can be viewed as confined to one side of the well. Each succeeding level has an increasingly higher tunneling probability, until in the vicinity of the barrier top the probability of proton tunneling becomes nearly 1. Here, the proton tunnels faster than the frequencies of the rest of the lattice, owing to its smaller mass. For convenience, the treatment below assumes only the existence of a ground state (the nontunneling level) and one other state right below the intrabond barrier (the fast tunneling level).

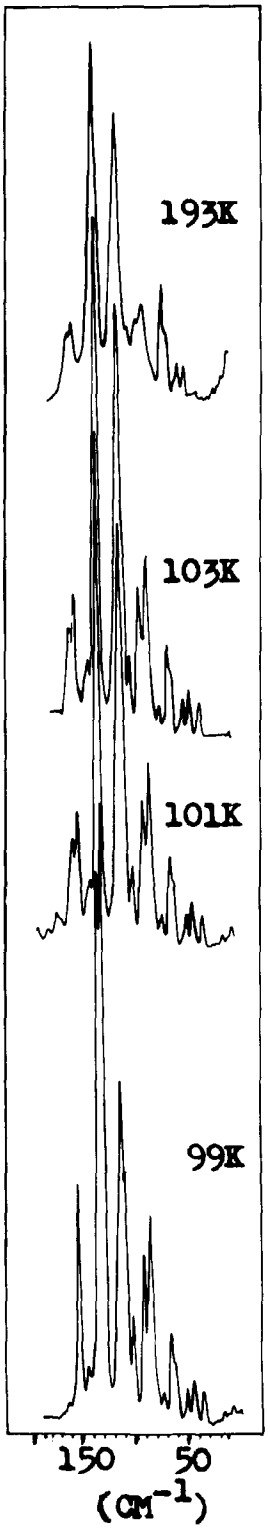

Three important restrictions on this description must be noted. First, the intrabond barrier is quite small, ~600 cm^{-1} above the ground state (*25*). Second, the separation between the slow and fast tunneling levels could be as small as 50 to 200 cm^{-1}. This assumption is made because the fast tunneling level must be populated at moderate temperatures (~150–300°K) to account for the disordered phase. Third, the fast tunneling of protons is a cooperative phenomenon only within very small regions of the crystal.

The disordered phase of the crystal can now be described as having the majority of its protons thermally populating the fast tunneling level, producing a symmetric proton density and consequently a more symmetric crystal structure. The SeO_3^{2-} ions view these protons in average positions, and the spectra are characteristic of $*SeO_3^{2-}$ ions with broad internal modes. The ordered phase of the crystal consists of the majority of protons in the nontunneling ground level; the SeO_3^{2-} ions view these protons as confined to one side of the well, producing characteristic $HSeO_3^-$ or H_2SeO_3 frequencies.

The "critical" slowing down of proton tunneling in the immediate vicinity of the ordered phase, as reported by NMR experiments (*25*), arises from a rapid shift in proton population between the levels. The tunneling frequencies in such cases represent the numerical average between the number of protons in the fast tunneling and nontunneling levels. Thus, the thermal population of levels is described and controlled by (at extreme temperature levels) a Boltzmann-like distribution function. Far above or below T_c a "normal" population is predicted; however, the cooperative nature of the tunneling motion causes a rapid shift in population near T_c, i.e., a cascade. The temperature spread of a second-order phase transition is directly gov-

FIG. 6. The $b(cb)a$ Raman spectrum of the lattice region of $NaH_3(SeO_3)_2$ in the $\beta \rightarrow \gamma$ phase transition temperature region.

erned by the energy separation of the levels and by the magnitude of the interaction between static and tunneling protons.

This approach to a theory of phase transitions in KDP-type crystals appears to be quite simple because the exact form of the coupling between tunneling protons, coupling between static and tunneling protons, and the temperature dependence of protons cascading between energy levels has been ignored. Inclusion of these terms in the model is extremely difficult because of the lack of experimental data. This model, therefore, is simplistic in its approach but is attractive because it correctly predicts many of the essential experimental facts.

In $NaH_3(SeO_3)_2$ protons occupy two different hydrogen bonds. Thus, the energy separation between the fast and nontunneling levels is expected to be different for each distinct hydrogen bond, and, therefore, from this description two different proton-triggered phase transitions are expected.

Spectroscopic evidence in support of the discrete energy level proposed here is based upon the behaviour of the hydrogen-bonded $*SeO_3^{2-}$ modes as a function of temperature. Upon passing into the ordered phase, if each proton has a temperature-dependent tunneling frequency, which slows down as the temperature is lowered, then the changing perturbation will continuously shift the $*SeO_3^{2-}$ frequencies until $HSeO_3^-$ or $H_2SeO_3^-$ frequencies dominate. However, as seen in Fig. 3, as one crosses the order–disorder transition, the intensities of the $*SeO_3^{2-}$ modes simply decrease, whereas those of the $HSeO_3^-$ modes increase. The spectra never indicate that proton tunneling has slowed down; quite the contrary is true: The spectra indicate that at a temperature of 193.3°K the crystal has some proton population in the fast tunneling level and some proton population in the static level.

Additional support for this point comes from the behavior of the spontaneous polarization with temperature. For second-order phase transitions, the polarization continuously increases, below T_c, as the temperature decreases. This result is due to the buildup of the ground level population, and in fact the final "saturated" polarization value represents a crystal with nearly the entire population of protons resting in the ground state.

At present, the actual shape of the proton potential well is an ambiguous question. Neutron and X-ray diffraction, along with NMR and DMR experiments, suggest that in many KDP-type crystals the well is a symmetric double-minimum type. However, the same experimental interpretation can be derived on the basis of an asymmetric well if the rapid proton tunneling averages out the asymmetry in the disordered phase. We favor the asymmetric case since it readily accounts for the above-described mechanism of the transition and yet removes the unnecessary assumption of a symmetric double minimum.

The well-known deuterium temperature shift for a proton-triggered phase transition is also readily explained by this model. The original fast tunneling level will drop down into the well upon deuteration and become a nontunneling level by virtue of the fact that it now lies quite far below the intrabond barrier top. To populate a fast tunneling level (say the third or fourth level above the ground state) to form the disordered phase, a much higher temperature must be reached.

Hydrogen Bond Stretching Region

The presence of an intrabond barrier in KDP-type crystals (MH_2PO_4, MH_2AsO_4, $MH_3(SeO_3)_2$, etc., where M = Li, Na, K, Cs, and Rb) has been ussed as the main criterion controlling the number, frequency, and breadth of the hydrogen-bonded O–H stretching bands of these compounds (*26*, *27*). However, several valid criticisms of these interpretations can be advanced. For instance, to calculate frequencies close to those observed in KH_2PO_4 (2800, 2400, and 1750 cm^{-1}) the intrabond barrier must be ~3300 cm^{-1} above the ground state (*26*). An intrabond

barrier of this magnitude eliminates any possibility of an order–disorder phase transition at moderate temperatures (50–300°K). Furthermore, the calculated frequencies are in poor numerical agreement with those observed, and also, typical measured intrabond barriers are generally about 600 cm^{-1} (*25*). These calculations are also inadequate in their prediction that at least one mode's intensity is temperature dependent.

Perhaps the severest criticism of these approaches comes from the realization that KDP-type crystals displaying a wide variance in hydrogen bond lengths, geometries, and phase transition behavior should have corresponding wide variances in calculated O–H stretching frequencies, intensities, and bandwidths, when in fact these same compounds have remarkably similar stretching regions (*28*).

Because of these difficulties, we believe that two nearly independent processes, one controlling the phase transition and another controlling the structure of the O–H stretching region, are responsible for these effects.

Schmidt and Uelhig (*25*) were the first to note that two independent proton tunneling processes were occurring in KD_2PO_4: a slow interbond tunneling (diffusion between hydrogen bonds) which was unaffected upon crossing T_c, and a fast intrabond tunneling (within a hydrogen bond) which critically slowed down as T_c was crossed. It is plausible, therefore, that the barrier controlling proton diffusion controls the number, breadth, and frequencies of the O–H stretching modes, and that the intrabond barrier controls the mechanism and nature of the phase transition. This description is very reasonable in view of the experimental data: First, the diffusion barriers of KDP-type crystals are similar in magnitude (4000–6000 cm^{-1}) (*29*), and thus the structure of the O–H stretching region of these crystals should be similar. Second, the diffusion barrier top lies in close proximity to an excited state and, therefore, may result in a large splitting of states which could explain the observed multiplicity. Because the large splitting occurs in an excited state no thermal depopulation (which would cause intensity changes) of these levels is anticipated upon cooling. Third, a normal deuteration shift of $\nu_D/\nu_H = 0.707$ is predicted and has been observed in KDP-type crystals. Fourth, the lack of any significant change in frequency, intensity, or bandwidth of the O–H stretching modes upon crossing below T_c, regardless of the transition type, arises because of the independence of the diffusion barrier with respect to the phase transition. Fifth, the abnormal bandwidths of these modes are due to long-range well-to-well diffusion coupling. Along these lines, previous researchers have noted that low concentrations ($\sim$1–5%) of deuterated species in their undeuterated hosts lead to sharp O–D bands (*30–32*). At higher concentrations, the bands markedly broaden, indicating the onset of coupling. This illustrates that the large breadth of these bands in the spectra of pure compounds cannot be due to the dynamics of individual wells but must arise from well-to-well coupling.

A more elaborate discussion of the diffusion barrier O–H stretching region hypothesis can be found in an earlier publication (*33*).

Conclusion

The infrared and Raman spectra of the ferroelectric phases of $NaH_3(SeO_3)_2$ and $NaD_3(SeO_3)_2$ are extremely complicated because of the large number of molecules in the unit cell and the low symmetry of each phase. The assignments presented in this article are of a tentative nature and should be refined by a complete study of the infrared and Raman spectra of H_2SeO_3, $NaHSeO_3$, and deuterated analogs. An understanding of the spectral properties of these compounds would greatly aid in assigning the internal and lattice mode region of $NaH_3(SeO_3)_2$ and determining the frequency, polarization properties, and atomic motions of the tunneling normal mode. Studies of this nature are presently being carried out.

The nonexistence β_D phase of $NaD_3(SeO_3)_2$ illustrates the changing hydrogen bond dynamics upon deuteration. Under the proposed phase transition mechanism the fast tunneling level drops down farther into the potential well and becomes nontunneling, because of the increased hydrogen bond length and deuteron mass. Offsetting these factors are variations in deuteron coupling efficiency in the new fast tunneling levels at higher energy. These factors working in combination could readily account for the anisomorphism of the $NaH_xD_{3-x}(SeO_3)_2$ solid solution series.

References

1. J. C. SLATER, *J. Chem. Phys.* **9**, 16 (1941).
2. G. E. BACON AND R. S. PEASE, *Proc. Roy. Soc. London, Ser. A* **230**, 359 (1955).
3. F. JONA AND G. SHIRANE, "Ferroelectric Crystals," Chap. 3, Macmillan, New York (1962).
4. P. S. PEERCY, *Opt. Commun.* **2**, 270 (1970).
5. R. PEPINSKY AND K. VEDAM, *Phys., Rev.* **114**, 1217 (1959).
6. A. A. SILVIDI AND D. T. WORKMAN, *J. Chem. Phys.* **55**, 4672 (1971).
7. R. BLINC AND M. PINTAR, *J. Chem. Phys.* **54**, 1535
8. Y. MAKITA, *J. Phys. Soc. Japan* **19**, 576 (1964).
9. G. SODA AND T. CHIBA, *J. Phys. Soc. Japan* **26**, 723 (1969).
10. R. K. KHANNA, J. C. DECIUS, AND E. R. LIPPINCOTT, *J. Chem. Phys.* **43**, 2974 (1965).
11. M. VIJAYAN, *Acta Crystallogr. B* **24**, 1237 (1968).
12. S. F. KAPLAN, M. I. KAY, AND B. MOROSIN, *Ferroelectrics* **1**, 1 (1970).
13. B. BLINC, J. STEPISNIK, AND I. ZUPANCIC, *Phys. Rev.* **176**, 732 (1968).
14. B. H. TORRIE AND R. R. KNISPEL, *Ferroelectrics* **5**, 5 (1973).
15. P. K. ACHARYA AND P. S. NARAYANAN, *Spectrochim. Acta A* **29**, 925 (1973).
16. C. A. CODY, R. C. LEVITT, R. S. VISWANATH, AND P. J. MILLER, *J. Solid State Chem.* **26**, 281 (1978).
17. L. A. SHUVALOV AND N. R. IVANOV, *Phys. Status Solidi* **22**, 279 (1967).
18. R. BLINC, A. JOVANOVIC, A. LEVSTIK, AND A. PRESLESNIK, *J. Phys. Chem. Solids* **26**, 1359 (1965).
19. E. V. PESHKIOV AND L. A. SHUVALOV, *Sov. Phys.-Crystall.* **18**, 499 (1974).
20. R. BLINC, A. LEVSTIK, J. STEPISNIK, S. TRONTELJ, AND I. AUPANCIC, *Phys. Lett. A* **26**, 290 (1968).
21. J. STEPISNIK, J. SLAK, R. BLINC, L. A. SHUVALOR, N. R. IVANOV, AND N. M. SCHAGINA, *Solid State Commun.* **13**, 1053 (1973).
22. Y. MAKITA AND H. MIKI, *J. Phys. Soc. Japan* **28**, 1221 (1970).
23. J. C. SLATER, *in* "Ferroelectricity" (E. F. Weller, Ed.), p. 1, Elsevier, Amsterdam (1967).
24. L. A. SHUVALOR, H. M. SHIROKOV, N. R. IVANOV, AND A. I. VARANOV, *Sov. Phys.-Crystall.* **18**, 80 (1963).
25. V. SCHMIDT AND E. UEHLING, *Phys. Rev.* **126**, 447 (1962).
26. R. L. SOMORJAI AND D. F. HORNING, *J. Chem. Phys.* **36**, 1980 (1962).
27. R. BLINC AND D. HADZI, *Mol. Phys.* **1**, 391 (1958).
28. C. A. CODY, Ph.D dissertation, University of Maryland (1976).
29. R. BLINC AND J. PIRS, *J. Chem. Phys.* **54**, 1535 (1971).
30. A. B. DEMPSTER AND G. ZERBI, *J. Chem. Phys.* **54**, 3600 (1971).
31. C. HAAS AND D. F. HORNING, *J. Chem. Phys.* **32**, 1763 (1960).
32. J. E. BERTIE AND E. WHALLEY, *J. Chem. Phys.* **40**, 1637 (1964).
33. C. A. CODY AND R. K. KHANNA, *Ferroelectrics* **9**, 25 (1975).